MEDIAN ROBUST EXTENDED LOCAL BINARY PATTERN FOR TEXTURE CLASSIFICATION

[1]*Li Liu*, [2]*Paul Fieguth*, [3]*Matti Pietikäinen*, [4] *Songyang Lao*

[1,4] School of Information System and Management, National University of Defense Technology, Changsha, China 410073
[2]Department of Systems Design Engineering, University of Waterloo, Waterloo, Canada N2L 3G1
[3]Center for Machine Vision Research, Department of Computer Science and Engineering, University of Oulu,90014 Oulu, Finland
Email:lilyliu_nudt@163.com, pfieguth@uwaterloo.ca, matti.pietikainen@ee.oulu.fi,feiyunlyi@hotmail.com

ABSTRACT

Local Binary Patterns (LBP) are among the most computationally efficient amongst high-performance texture features. However, LBP is very sensitive to image noise and is unable to capture macrostructure information. To best address these disadvantages, in this paper we introduce a novel descriptor for texture classification, the Median Robust Extended Local Binary Pattern (MRELBP). In contrast to traditional LBP and many LBP variants, MRELBP compares local image medians instead of raw image intensities. We develop a multiscale LBP-type descriptor by efficiently comparing image medians over a novel sampling scheme, which can capture both microstructure and macrostructure. A comprehensive evaluation on benchmark datasets reveals MRELBP's remarkable performance (robust to gray scale variations, rotation changes and noise) relative to state-of-the-art algorithms, but nevertheless at a low computational cost, producing the best classification scores of 99.82%, 99.38% and 99.77% on three popular Outex test suites. Furthermore, MRELBP is also shown to be highly robust to image noise including Gaussian noise, Gaussian blur, Salt-and-Pepper noise and random pixel corruption.

Index Terms— Texture classification, Feature extraction, Local binary pattern, Local descriptors, Median filtering

1. INTRODUCTION

Texture is an important characteristic of many types of images. It can be seen in images ranging from multispectral remotely sensed data to microscopic images. Local Binary Patterns (LBP) [1] have emerged as one of the most prominent texture descriptors and have attracted significant attention in the field of computer vision and image analysis due to their outstanding advantages: (1) ease of implementation, (2) invariance to monotonic illumination changes, and (3) low computational complexity. Although originally proposed for texture analysis, the LBP method has been successfully applied to diverse problems including dynamic texture recognition, remote sensing, fingerprint matching, image retrieval, biomedical image analysis, face image analysis, motion analysis, and environment modeling [2–7]. Due to this progress, the division between texture descriptors and more generic image or video descriptors has been disappearing. Consequently a large number of LBP variants have been developed to improve its robustness, discriminative power, and breadth of applicability.

In terms of discriminative power, significant LBP variants include the Completed Local Binary Pattern (CLBP) [8], Extended Local Binary Pattern (ELBP) [6], Discriminative Completed Local Binary Pattern (*dis*CLBP) [9], Pairwise Rotation Invariant Cooccurrence Local Binary Pattern (PRICoLBP) [7] and the combination of Dominant Local Binary Pattern (DLBP) and Gabor filtering features [10]. However, despite the increase in discriminativeness, these LBP variants suffer in terms of robustness, as they have minimal tolerance to image blur and noise corruption, as well as increased computational complexity and feature dimensionality. Similar, with respect to LBP sensitivity to image degradation caused by blurring and random noise, significant variations include the Local Ternary Pattern (LTP) [11], Median Binary Pattern (MBP) [12], Local Phase Quantization (LPQ) [13], Fuzzy Local Binary Pattern (FLBP) [14], Noise Tolerant Local Binary Pattern (NTLBP) [15], Robust Local Binary Pattern (RLBP) [16] and Noise Resistant Local Binary Pattern (NRLBP) [17]. Although more robust than traditional LBP, the noise tolerance of these methods is still unsatisfactory, and in some cases the methods compromise discriminative power or impose a heavy computation burden.

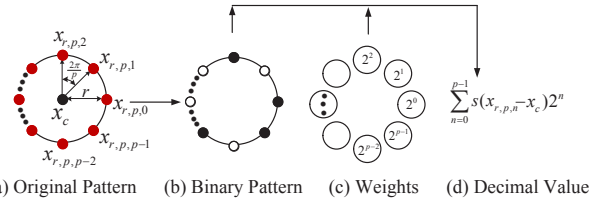

(a) Original Pattern (b) Binary Pattern (c) Weights (d) Decimal Value

Fig. 1. (a) A typical (r, p) neighborhood type used to derive a LBP like operator: central pixel x_c and its p circularly and evenly spaced neighbors $x_0, \cdots, x_{p-1}$ on a circle of radius r.

We previously developed the ELBP approach [6], in which four LBP-like descriptors — Center Intensity based LBP (ELBP_CI), Neighborhood Intensity based LBP (ELBP_NI), Radial Difference based LBP (ELBP_RD) and Angular Difference based LBP (ELBP_AD)[1] — were proposed. It was shown that the joint probability distribution of ELBP_CI, ELBP_NI and ELBP_RD (collectively referred as ELBP) produces good texture classification performance, however with disadvantages of (i) sensitivity to image blur and noise, (ii) failing to capture texture macrostructure, and (iii) having high feature dimensionality. In order to overcome these shortcomings, in this paper we propose a theoretically very simple, high-quality, yet efficient multiresolution approach, the Median Robust Extended Local Binary Pattern (MRELBP). The proposed MRELBP approach possesses some attractive attributes: (1) Gray-scale invariance, (2)

*This work has been supported by the National Natural Science Foundation of China under contract No. 61202336 and No. 61201339.

[1] In the original work [6], ELBP_CI, ELBP_NI, ELBP_RD and ELBP_AD are referred to as CI-LBP, NI-LBP, RD-LBP and AD-LBP respectively.

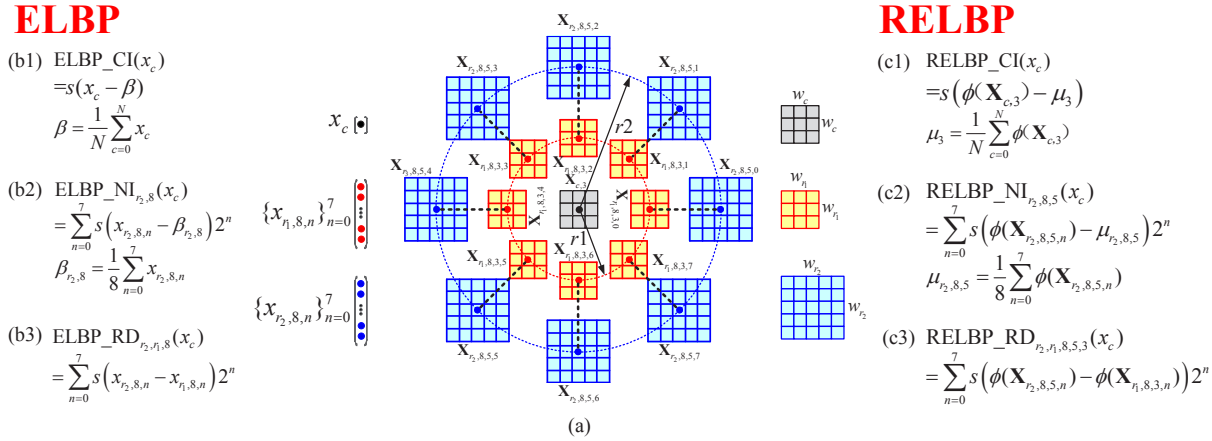

Fig. 2. Illustration for the proposed MRELBP descriptor on radius r_2 given a center pixel x_c. The key differences between the ELBP [6] and the MRELBP is that the only single pixel values are used in the ELBP, as opposed to a windowed / scaled / median approach in the MRELBP.

Rotation invariance, (3) No need for pretraining, (4) No parameter tuning, (5) Strong Discriminativeness, (6) Strong noise robustness, and (7) Computational efficiency.

The remainder of this paper is organized as follows. The derivation of the proposed approach operators and the classification framework are described in Section 2, and experimental results are presented in Section 3.

2. MEDIAN ROBUST EXTENDED LOCAL BINARY PATTERN

2.1. A Brief Review of LBP

The local binary pattern proposed by Ojala *et al.* [1] characterizes the spatial structure of a local image patch by encoding the differences between the pixel value of the central point and those of its neighboring points, considering only the sign information to form a local binary pattern. The corresponding decimal value of the generated binary pattern is then used to label the given pixel. Formally, as illustrated in Fig. 1, given a pixel x_c in the image, the LBP response is calculated by comparing its value with those of its p neighboring pixels that are evenly distributed in angle on a circle of radius r centered at center c:

$$\text{LBP}_{r,p}(x_c)=\sum_{n=0}^{p-1}2^n\,s(x_{r,p,n}-x_c),\;\; s(x)=\begin{cases}1 & x\geq 0\\ 0 & x<0\end{cases} \qquad (1)$$

where $s()$ is the sign function. Relative to the origin at $(0,0)$ of the central pixel, the coordinates of the neighbors are given by $(-r\sin(2\pi n/p), r\cos(2\pi n/p))$. The gray values of neighbors which do not fall exactly in the center of pixels are estimated by interpolation. A texture image can then be characterized by the probability distribution of the 2^p LBP patterns. To be able to include textural information at different scales, the LBP operator was later extended to use different radii [1], with values of (r,p) often selected as $(1,8),(2,16),(3,24)$.

Ojala *et al.* [1] observed that certain LBP patterns represent the fundamental texture microstructures, and named these patterns uniform patterns. Precisely, an LBP pattern is called uniform if it has a U value of at most two:

$$U(\text{LBP}_{r,p})=\sum_{n=0}^{p-1}|s(x_{r,p,n}-x_c)-s(x_{r,p,\text{mod}(n+1,p)}-x_c)|, \qquad (2)$$

where the $U(\text{LBP}_{r,p})$ represents the bitwise transitions from 0 to 1 or vice versa. Therefore the uniform descriptor, denoted as $\text{LBP}^{u2}_{r,p}$, has $p(p-1)+3$ categories consisting of $p(p-1)+2$ distinct uniform patterns and one nonuniform group containing all nonuniform patterns.

In order to gain rotation invariance and to obtain low feature dimensionality, Ojala *et al.* [1] proposed to further group the uniform patterns into $p+1$ different rotation-invariant categories, leading to the rotation invariant uniform descriptor $\text{LBP}^{riu2}_{r,p}$ with a much lower dimensionality of $p+2$:

$$\text{LBP}^{riu2}_{r,p}=\begin{cases}\sum_{n=0}^{p-1}s(x_{r,p,n}-x_c), & \text{if } U(\text{LBP}_{r,p})\leq 2\\ p+1, & \text{otherwise}\end{cases} \qquad (3)$$

2.2. Proposed MRELBP Descriptor

One problem with ELBP [6] is that it is very vulnerable to image noise, therefore the first strategy is to replace individual pixel intensities at a point with the representative over a region. Noticeable parallel methods along these lines include BRIEF [21], BRISK [19] and FREAK [20], where a binary descriptor vector is obtained by comparing the intensities of a number of pairs of pixels after applying a Gaussian smoothing or averaging smoothing to reduce the noise sensitivity. However, BRIEF, BRISK and FREAK are designed for image matching. Furthermore, a single pixel with a very unrepresentative or corrupted noise, can significantly affect the Gaussian smoothed value or average value of all the pixels in its neighborhood, resulting in an unreliability of the binary code. Therefore, we propose Median Robust Extended Local Binary Pattern (MRELBP) where we replace the raw pixel values with the median derived from local patches.

The ELBP descriptor [6] is now modified so that individual pixel intensities at the sampled points are replaced by median values, as highlighted in Fig. 2, where $\phi(\mathbf{X}_{r,p,w_r,n})$ is the median of all the pixels in the local patch $\mathbf{X}_{r,p,w_r,n}$ centered on $x_{r,p,n}$. To make comparison as objective and clear as possible, all other preprocessing and postprocessing steps are maintained consistent with ELBP: Images normalized to zero mean and unit variance, standard encoding scheme (^{riu2}) is used, joint histograms of MRELBP_CI, $\text{MRELBP\_NI}^{riu2}_{r,p}$ and $\text{MRELBP\_NI}^{riu2}_{r,p}$ are used to represent a textured image. This new descriptor is referred to as $\text{MRELBP}^{riu2}_{r,p}$.

Formally, the proposed new MRELBP_CI, MRELBP_NI and MRELBP_RD descriptors are defined as follows, as illustrated in Fig. 2:

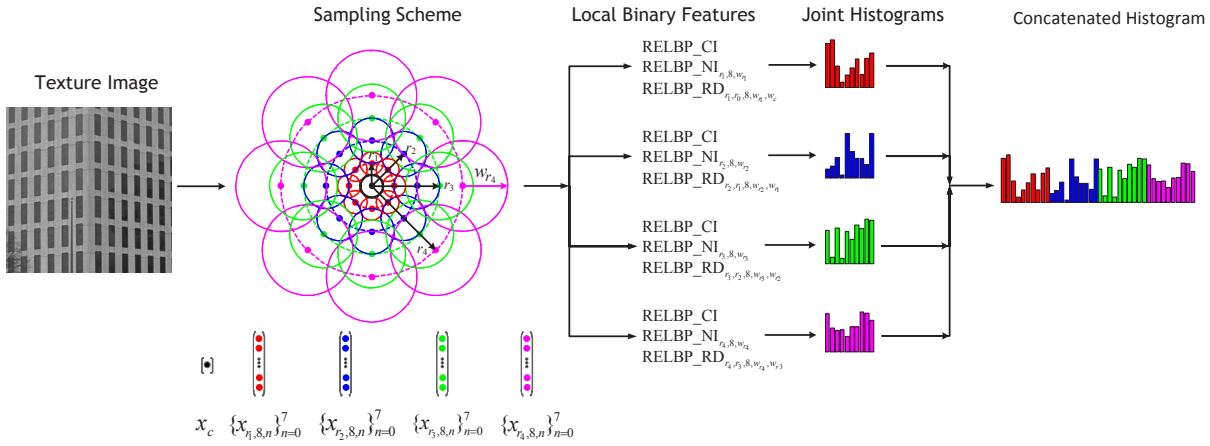

Fig. 3. Overview of the proposed multiscale MRELBP descriptor. Each solid circle represents a region which is represented by a local median. While this pattern resembles DAISY [18], BRISK [19] and FREAK [20], it is important to note that its use in the proposed MRELBP is entirely different, as DAISY [18] was built specifically for dense matching, and BRISK [19] and FREAK [20] were designed for image matching. Furthermore, DAISY, BRISK and FREAK applied Gaussian smoothing or mean smoothing.

1. MRELBP_CI

$$\text{MRELBP\_CI}(x_c) = s\big(\phi(\mathbf{X}_{c,w}) - \mu_w\big) \tag{4}$$

where $\mathbf{X}_{c,w}$ denotes the local patch of size $w \times w$ centered at the center pixel x_c under consideration, the function $\phi(\mathbf{X})$ is the median value over $\mathbf{X}$ and μ_w is the mean of $\phi(\mathbf{X}_{c,w})$ over the whole image.

2. MRELBP_NI

$$\begin{aligned}&\text{MRELBP\_NI}_{r,p}(x_c)\\ &= \textstyle\sum_{n=0}^{p-1} s\big(\phi(\mathbf{X}_{r,p,w_r,n}) - \mu_{r,p,w_r}\big)2^n\\ &\mu_{r,p,w_r} = \frac{1}{p}\textstyle\sum_{n=0}^{p-1}\phi(\mathbf{X}_{r,p,w_r,n})\end{aligned}$$

where $\mathbf{X}_{r,p,w_r,n}$ denotes the patch of size $w_r \times w_r$ centered at the neighboring pixel $x_{r,p,n}$.

3. MRELBP_RD

$$\begin{aligned}&\text{MRELBP\_RD}_{r,r-1,p,w_r,w_{r-1}}\\ &= \textstyle\sum_{n=0}^{p-1} s\big(\phi(\mathbf{X}_{r,p,w_r,n}) - \phi(\mathbf{X}_{r-1,p,w_{r-1},n})\big)2^n\end{aligned}$$

where $\mathbf{X}_{r,p,w_r,n}$ denotes the patches centered at the neighboring pixels $x_{r,p,n}$, which are the circularly and evenly spaced neighbors of the center pixel x_c on radius r.

2.3. MultiScale Analysis and Classification

Like most LBP variants, by altering r and p, we can realize operators for any quantization of the angular space and for any spatial resolution. A multiresolution analysis can be accomplished by concatenating binary histograms from multiple resolutions into a single histogram, clearly requiring that the histogram feature produced at each resolution be of low dimension.

The feature dimensionality of the proposed MRELBP$^{riu2}_{r,p}$ is 2(p+2)(p+2). If we follow most LBP variants by adopting (r,p) as (2,8)(4,16)(6,24)(8,24), a four-scale MRELBP$^{riu2}_{r,p}$ descriptor results with a feature dimensionality of 3552. In order to reduce the number of bins we keep the number of sampling neighbors p at each scale at a constant *eight*, in which case MRELBP$^{riu2}_{r,8}$ has 200 bins. Furthermore, following BRISK [19] and FREAK [20], in order to avoid aliasing effects when sampling the image, the patch size $w_r \times w_r$ associated with the median operator is set to be proportional to radius r instead of being fixed, leading to the multiscale sampling scheme illustrated in Fig. 3. While this pattern resembles the DAISY [18], BRISK [19] and FREAK [20], it is important to note that its use in MRELBP is entirely different, as they all applied Gaussian smoothing and DAISY [18] was built specifically for dense matching, and BRISK [19] and FREAK [20] were designed for image matching.

In terms of the overall famework of the proposed approach, the actual classification is performed via the simple Nearest Neighbor Classifier (NNC), applied to the normalized MRELBP histogram feature vectors, using the χ^2 distance metric as in [8, 22, 23].

3. EXPERIMENTAL EVALUATION

3.1. Image Data and Experimental Setup

By selecting 24 different homogeneous texture classes from the Outex database [27], Ojala *et al.* [1] created three test suites, named Outex_TC10, Outex_TC12_000 and Outex_TC12_001, which have been widely used as benchmark datasets for the evaluation of rotation and illumination invariant texture classification approaches. The major difference between these three test suites is in the type of variations and level of difficulty. Outex_TC10 contains testing images that are different from training images only with respect to changes in degree of rotation while Outex_TC12_000 and Outex_TC12_001 contain testing images that are different from training images with respect to both illumination conditions and degrees of rotation.

In order to measure the noise tolerance of our approach, we have used a challenging experimental setup by taking texture images without noise as training set and utilizing the training data added with noise of different levels as testing. We have considered four different types of noise: additive Gaussian noise, Gaussian blur, random Salt-and-Pepper noise and random pixel corruption[2], leading to a number of test suites, all having the same training images.

The testing images in Outex_TC11n[3] have additive Gaussian noise with standard deviation $\sigma = 5$. For Outex_TC11b, the testing images were artificially blurred using a Gaussian PSF with standard deviations σ of $\{0.5, 0.75, 1, 1.25\}$, which mimics the blur caused, for example, by atmospheric turbulence. For Outex_TC11s, the testing images were corrupted with random Salt-and-Pepper noise with

[2]This is the same noise type tested in [28]

[3]Outex_TC11n can be download at "http://lagis-vi.univ-lille1.fr/datasets/outex.html"

Table 1. Classification scores (%) on noisy test suites Outex_TC11n, Outex_TC11b, Outex_TC11s and Outex_TC11c, comparing the proposed approach with eleven state of the art LBP variants. Observe the major improvement right across the board, for all types and levels of noise.

Robust to	Gaussian Noise	Gaussian Blur				Salt-and-Pepper Noise Robustness							Robustness to Random Corrupted Pixels				
Datasets	Outex_TC11n	Outex_TC11b				Outex_TC11s							Outex_TC11c				
Method	$\sigma = 5$	$\sigma = 0.5$	$\sigma = 0.75$	$\sigma = 1$	$\sigma = 1.25$	ρ =5%	ρ =10%	ρ =15%	ρ =20%	ρ =30%	ρ =40%	ρ =50%	$\upsilon = 5\%$	$\upsilon = 10\%$	$\upsilon = 20\%$	$\upsilon = 30\%$	$\upsilon = 40\%$
MRELBP$^{riu2}_{r,p}$	**91.5**	**100.0**	**100.0**	**93.8**	**75.4**	**100.0**	**100.0**	**100.0**	**100.0**	**100.0**	**85.8**	**50.2**	**100.0**	**100.0**	**100.0**	**99.6**	**90.6**
LBP$^{riu2}_{r,p}$ [1]	12.7	89.0	45.4	22.5	12.1	38.5	4.4	4.2	4.2	4.2	4.2	4.2	53.1	9.8	4.2	4.2	4.2
ELBP$^{riu2}_{r,p}$ [6]	12.3	100.0	72.7	40.8	17.7	31.9	10.4	6.7	4.2	4.2	4.2	4.2	66.7	30.8	12.3	6.0	4.2
CLBP$^{riu2}_{r,p}$ [8]	13.5	99.8	81.7	52.9	24.0	10.6	7.7	7.9	8.3	4.2	4.2	4.2	72.7	29.2	4.2	4.2	4.2
MBP$^{riu2}_{r,p}$ [12]	11.7	67.9	18.8	12.7	8.3	29.6	11.7	8.3	6.9	4.2	4.2	4.2	39.8	17.1	8.3	4.8	4.2
NTLBP$^{new}_{r,p}$ [15]	15.6	82.1	39.0	26.0	17.3	53.3	27.5	13.5	11.3	5.4	4.2	4.2	64.4	36.0	8.3	8.3	8.3
PRICoLBP$_g$ [7]	15.4	98.1	50.0	26.5	14.4	9.6	8.1	5.2	4.2	4.2	4.2	4.2	31.7	10.0	4.2	4.2	4.2
LTP$^{riu2}_{r,p}$ [11]	8.5	88.3	37.7	17.7	8.8	10.2	4.2	4.2	6.5	8.3	4.2	4.2	49.0	17.5	8.1	4.2	4.2
NRLBP$^{riu2}_{r,p}$ [17]	11.7	85.4	29.4	14.2	9.4	5.8	5.8	4.2	4.2	5.2	5.6	4.2	50.8	29.0	16.7	11.7	4.2
MSJLBP [24]	17.7	96.0	46.0	26.0	11.9	14.2	10.2	8.3	8.3	4.4	4.2	4.2	32.3	16.7	7.5	4.2	4.2
dis(S+M)$^{ri}_{r,p}$ [25]	15.8	97.1	62.3	35.6	19.6	18.5	4.4	5.8	8.3	4.2	4.2	4.2	45.0	18.5	4.2	4.2	4.2
COV-LBPD [26]	23.5	99.2	86.9	65.6	46.0	27.1	13.8	8.3	7.7	4.2	4.2	4.2	26.9	17.7	8.5	4.6	4.2

Table 2. Comparing the classification scores (%) achieved by the proposed approach with those achieved by recent state-of-the-art texture classification methods on the three Outex test suites. Scores are as originally reported, except those marked ($\diamond$) which are taken from the work by Guo *et al.* [8] and those marked ($\star$) which are obtained according our own implementation. For CLBP, LBPD and PRICoLBP$_g$, we used the code provided by the authors.

Method	TC10	TC12		Mean	Reference	Feature Dimension
		tl84	horizon			
MRELBP$^{riu2}_{r,p}$	**99.82**	**99.38**	**99.77**	**99.65**	This Paper	800
LBP$^{riu2}_{r,p}$ · VAR$_{r,p}$ [1]	97.7	87.3	86.4	90.47	TPAMI 2002	864
VZ-MR8 [29]	93.59($\diamond$)	92.55($\diamond$)	92.82($\diamond$)	92.99($\diamond$)	IJCV 2005	960
MBP$^{riu2}_{r,p}$ [12]	89.92	95.18	95.55	96.62	ICIAR 2007	108
FLBP$^{riu2}_{r,p}$ [14]	97.53($\star$)	90.32($\star$)	86.87($\star$)	91.57($\star$)	ICIAR 2008	60
VZ-Patch [30]	92.00($\diamond$)	91.41($\diamond$)	92.06($\diamond$)	91.82($\diamond$)	TPAMI 2009	960
CLBP$^{riu2}_{r,p}$ [8]	99.14	95.18	95.55	96.62	TIP 2010	2200
LTP$^{riu2}_{r,p}$ [11]	98.54($\star$)	92.59($\star$)	89.17($\star$)	93.43($\star$)	TIP 2010	108
LBPV$^{u2}_{r,p}$GM$^{P/2-1}_{\text{PD2}}$ [22]	97.63	95.06	93.88	95.52	PR 2010	2211
CLBC [9]	98.96	95.37	94.72	96.35	TIP 2012	1990
dis(S+M)$^{ri}_{r,p}$ [25]	98.93($\star$)	97.0	96.5	97.48	PR 2012	2668
NTLBP$^{new}_{r,p}$ [15]	99.24	96.18	94.28	96.57	PRL 2012	108
NRLBP$^{riu2}_{r,p}$ [17]	93.44	86.13	87.38	88.98	TIP 2013	30
MSJLBP [24]	96.67($\star$)	95.21($\star$)	95.74($\star$)	95.87($\star$)	BMVC 2013	3540
PRICoLBP$_g$ [7]	94.48($\star$)	92.57($\star$)	92.50($\star$)	93.18($\star$)	TPAMI 2014	3540
COV-LBPD [26]	98.78($\star$)	95.72($\star$)	97.62($\star$)	97.37($\star$)	TIP 2014	289

densities ρ in $\{5\%, 10\%, 15\%, 20\%, 30\%, 40\%, 50\%\}$. For Outex_TC11c, we corrupted certain percentage of randomly chosen pixels from each of the images, replacing their values with independent and identically distributed samples from a uniform distribution [4]. The corrupted pixels are randomly chosen for each test image, and the locations are unknown to the algorithm. We vary the percentage of corrupted pixels υ as $\{5\%, 10\%, 20\%, 30\%, 40\%\}$.

The main parameters involved in the proposed descriptor are the sampling radii r, the size $w_c \times w_c$ of the center patch, and the sizes $w_r \times w_r$ of the neighboring patches. Extensive experiments regarding these parameter choices have been conducted, however the results are not shown due to space limitation. We find that choosing (r, p) as (2,8)+(4,8)+(6,8)+(8,8), $w_c = 3$ and $w_r = r + 1$ (shown in Fig. 3) give very good results, in general, and therefore will be our choice. For the state-of-the-art methods used in our comparison, we have used the recommended approaches and parameter settings in the respective papers.

3.2. Results

Table 2 compares the classification performance of the proposed MRELBP$^{riu2}_{r,p}$ descriptor with those of *fifteen* recent state of the art LBP variants on the three Outex benchmark test suites. We can observe that our MRELBP approach performs significantly and consistently better than all 15 methods. The striking performance of MRELBP$^{riu2}_{r,p}$ clearly demonstrates that the concatenated joint distributions of the proposed MRELBP_CI$^{riu2}_{r,p}$, MRELBP_NI$^{riu2}_{r,p}$ and MRELBP_RD$^{riu2}_{r,p}$ codes and the novel sampling scheme turns out to be a very powerful representation of image texture, demonstrating that the proposed approach can make effective use of both microstructure and macrostructures. To the best of our knowledge, the classification scores of 99.82%, 99.38% and 99.77% for our proposed approach are the best reported for Outex_TC10, Outex_TC12_000 and Outex_TC12_001. Keeping in mind the variations in gray scale and rotation present in the three test suites, the results in Table 2 firmly demonstrate the illumination and rotation invariance claimed of the MRELBP$^{riu2}_{r,p}$ approach. Table 2 also compares the feature dimensionality of the methods, where we can observe the modest feature dimensionality of the proposed approach, leading to savings in computational time and memory storage.

Finally, Table 1 gives the classification results for four different types of noise, to test the applicability of the texture feature to real-world applications. The table quite strikingly shows the strong noise robustness offered by the MRELBP$^{riu2}_{r,p}$ descriptor. There are difficult noise levels where the proposed approach still offers strong performance, but where not a single state-of-the-art method delivers acceptable results.

4. CONCLUSIONS

We have presented a novel MRELBP descriptor which outperforms all tested state-of-the-art LBP-type descriptors in noise free situations and demonstrates striking robustness to image noise including Gaussian white noise, Gaussian blur, Salt-and-Pepper and pixel random corruption. The proposed MRELBP has nice properties of computational simplicity, gray scale and rotation invariance, no need for a pretraining and no tuning of parameters. Future work includes examining higher level applications such as object recognition.

5. REFERENCES

[1] T. Ojala, M. Pietikäinen, and T. Maenpää, "Multiresolution gray-scale and rotation invariant texture classification with local binary patterns," *IEEE Trans. Pattern Anal. Mach. Intell.*, vol. 24, no. 7, pp. 971–987, Jul 2002.

[2] M. Pietikänen, A. Hadid, G. Zhao, and T. Ahonen, *Computer*

[4] Uniform over $[0,\ y_{max}]$, where y_{max} is the largest possible pixel value.

Vision Using Local Binary Patterns. London, UK: Springer, 2011.

[3] T. Ahonen, A. Hadid, and M. Pietikäinen, "Face decription with local binary patterns: application to face recognition," *IEEE Trans. Pattern Anal. Mach. Intell.*, vol. 28, pp. 2037–2041, July 2006.

[4] G. Zhao and M. Pietikäinen, "Dynamic texture recognition using local binary patterns with an application to facial expressions," *IEEE Trans. Pattern Anal. Mach. Intell.*, vol. 29, pp. 915–928, 2007.

[5] T. Ahonen, J. Matas, C. He, and M. Pietikäinen, "Rotation invariant image description with local binary pattern histogram fourier features," in *Proc. Scand. Conf. Image Anal.* IEEE, 2009, pp. 61–70.

[6] L. Liu, L. Zhao, Y. Long, G. Kuang, and P. Fieguth, "Extended local binary patterns for texture classification," *Image and Vision Computing*, vol. 30, pp. 86–99, 2012.

[7] X. Qi, R. Xiao, C. Li, Y. Qiao, J. Guo, and X. Tang, "Pairwise rotation invariant co-occurrence local binary pattern," *IEEE Trans. Pattern Anal. Mach. Intell.*, vol. 36, no. 11, pp. 2199–2213, November 2014.

[8] Z. Guo, L. Zhang, and D. Zhang, "A completed modeling of local binary pattern operator for texture classification," *IEEE Trans. Image Process.*, vol. 9, pp. 1657–1663, 2010.

[9] Y. Zhao, D. Huang, and W. Jia, "Completed local binary count for rotation invariant texture classification," *IEEE Trans. Image Process.*, vol. 21, pp. 4492–4497, October 2012.

[10] S. Liao, M. Law, and A. Chung, "Dominant local binary patterns for texture classification," *IEEE Trans. Image Process.*, vol. 18, pp. 1107–1118, 2009.

[11] X. Tan and B. Triggs, "Enhanced local texture feature sets for face recognition under difficult lighting conditions," *IEEE Trans. on Image Process.*, vol. 19, pp. 1635–1650, 2010.

[12] A. Hafiane, G. Seetharaman, and B. Zavidovique, "Median binary pattern for textures classification," in *Proceedings of the 4th International Conference on Image Analysis and Recognition*, 2007, pp. 387–398.

[13] V. Ojansivu, E. Rahtu, and J. Heikkilä, "Rotation invariant local phase quantization for blur insensitive texture analysis," in *IEEE International Conference on Pattern Recognition (ICPR)*, 2008, pp. 1–4.

[14] D. Iakovidis, E. Keramidas, and D. Maroulis, "Fuzzy local binary patterns for ultrasound texture characterization," in *Image Analysis and Recognition*, ser. Lecture Notes in Computer Science, A. Campilho and M. Kamel, Eds. Springer Berlin Heidelberg, 2008, vol. 5112, pp. 750–759.

[15] A. Fathi and A. Naghsh-Nilchi, "Noise tolerant local binary pattern operator for efficient texture analysis," *Pattern Recognit. Letters*, vol. 33, no. 9, pp. 1093–1100, 2012.

[16] J. Chen, V. Kellokumpu, G. Zhao, and M. Pietikänen, "Rlbp: robust local binary pattern," in *British Vision Conference on Computer Vision (BMVC)*, 2013.

[17] J. Ren, X. Jiang, and J. Yuan, "Noise-resistant local binary pattern with an embedded error-correction mechanism," *IEEE Trans. Image Process.*, vol. 22, no. 10, pp. 4049–4060, 2013.

[18] E. Tola, V. Lepetit, and P. Fua, "Daisy: An efficient dense descriptor applied to wide-baseline stereo," *IEEE Trans. Pattern Anal. Mach. Intell.*, vol. 32, no. 5, pp. 815–830, 2010.

[19] S. Leutenegger, M. Chli, and R. Siegwart, "Brisk: Binary robust invariant scalable keypoints," in *International Conference on Computer Vision (ICCV)*, 2011, pp. 2548–2555.

[20] A. Alahi, R. Ortiz, and P. Vandergheynst, "Freak: fast retina keypoint," in *Computer Vision and Pattern Recognition (CVPR)*. IEEE, 2012, pp. 510–517.

[21] M. Calonder, V. Lepetit, M. Ozuysal, T. Trzcinski, C. Strecha, and P. Fua, "Brief: computing a local binary descriptor very fast," *IEEE Trans. Pattern Anal. Mach. Intell.*, vol. 34, pp. 1281–1298, July 2012.

[22] Z. Guo, L. Zhang, and D. Zhang, "Rotation invariant texture classification using lbp variance (lbpv) with global matching," *Pattern Recognit.*, vol. 43, pp. 706–719, 2010.

[23] L. Liu and P. Fieguth, "Texture classification from random features," *IEEE Trans. Pattern Anal. Mach. Intell.*, vol. 34, no. 3, pp. 574 –586, March 2012.

[24] X. Qi, Y. Qiao, C. Li, and J. J. Guo, "Multiscale joint encoding of local binary patterns for texture and material classification," in *Proceedings of British Machine Vision Conference (BMVC)*, 2013.

[25] Y. Guo, G. Zhao, and M. Pietikäinen, "Discriminative features for texture description," *Pattern Recognit.*, vol. 45, pp. 3834–3843, 2012.

[26] X. Hong, G. Zhao, M. Pietikainen, and X. Chen, "Combining lbp difference and feature correlation for texture description," *IEEE trans. Image Process.*, vol. 23, no. 6, pp. 2557 – 2568, 2014.

[27] T. Ojala, T. Mäenpää, M. Pietikänen, J. K. J. Viertola, and S. Huovinen, "Outex–new framework for empirical evaluation of texture analysis algorithms," in *Proc. 16th Int. Conf. Pattern Recognit.*, 2002, pp. 701–706.

[28] J. Wright, A. Yang, A. Ganesh, S. Sastry, and Y. Ma, "Robust face recognition via sparse representation," *IEEE Trans. Pattern Anal. Mach. Intell.*, vol. 31, no. 2, pp. 210–227, 2009.

[29] M. Varma and A. Zisserman, "A statistical approach to texture classification from single images," *Int. J. Comput. Vision*, vol. 62, no. 1-2, pp. 61–81, 2005.

[30] ——, "A statistical approach to material classification using image patches," *IEEE Trans. Pattern Anal. Mach. Intell.*, vol. 31, no. 11, pp. 2032–2047, 2009.